

Chemically-inspired Memristor-based Neuron-like Oscillating Circuit

Theodoros Panagiotis Chatzinikolaou*, Iosif-Angelos Fyrigos*, Charalampos Tsiouostas†, Panagiotis Bousoulas†, Michail-Antisthenis Tsompanas*‡, Dimitris Tsoukalas†, and Georgios Ch. Sirakoulis*

* Department of Electrical and Computer Engineering, Democritus University of Thrace, Xanthi, Greece

† Department of Applied Physics, National Technical University of Athens, Athens, Greece

‡ Department of Computer Science and Creative Technologies, University of the West of England, Bristol, UK

Abstract—There is a constant push for ever increasing performance in traditional computing systems, leading to high power consumption and, in the end, to the incapacity of conventional electronics to handle heavy computing tasks, which usually require learning features. Thus, the development of novel nanoelectronic devices with inherent neuromorphic characteristics and a low energy footprint has become a viable alternative. In order to simulate neuromorphic features utilizing memristive devices, the threshold switching effect is critical, which can be seen in the rich dynamics of metallic conductive filament (CF). In this paper, a realistic model of the unipolar nature of CBRAM devices is exploited to create a memristor-based oscillator that can integrate neuromorphic features. Bipolar memristive devices have been used to match the weight of the neurons in a crossbar configuration. The used physical model for these memristors was fitted to fabricated devices in order to achieve the expected accuracy in the circuit simulation. The oscillator’s output signal and behavior matched the theoretical background of biological neurons. Thus, this approach can be considered as the first step towards the development of low-power oscillation-based neuromorphic hardware with biological-like behavior.

Index Terms—memristor, memristor oscillators, memristive circuits, neuromorphic computing, unconventional computing, oscillation-based computations

I. INTRODUCTION

Neuromorphic computing is one of the most promising novel computing approaches under investigation. Due to their ability to process complex data efficiently, neuromorphic systems have gained favor as the next generation of computing. Its definition focuses on the design of systems that can replicate the human brain, allowing them to attain high energy efficiency, parallelism, and competence in cognitive tasks such as object recognition and learning [1]–[3].

Neuromorphic systems were first introduced in the literature as a field of analog circuit engineering back in the 1980s. Over the years, analog circuits for neurons and synaptic functions have been created, leading to the production of general-purpose chip prototypes [1]. Although CMOS technology is required for the integration of large-scale neuromorphic systems, it lacks some of the inherent properties of the neurobiological network and has limitations in terms of power consumption and learning speed [4]–[6].

This work has been supported by the Hellenic Foundation for Research and Innovation (H.F.R.I.) under the “First Call for H.F.R.I. Research Projects to support Faculty members and Researchers and the procurement of high-cost research equipment grant” (Project Number: 3830).

An energy-efficient neuromorphic computing system demands hardware that can replicate brain activities. As a result, different materials for the designing of neuromorphic devices have been introduced [7]–[9]. Memristor as a two-terminal nonvolatile device has many advantages compared with conventional computing systems such as CPU and GPU [10], [11]. Due to its nanoscale size, its main characteristics focus on its low power consumption and rapid switching. It is also CMOS-compatible and can be integrated with higher density. These characteristics make the memristor suitable for a number of novel computing and memory applications [12]–[14] and, as such, a promising candidate for neuromorphic computing, enabling the mimicking of the energy-efficient signal system in the brain. Thus, researchers have conducted many experiments on neural networks in recent years using memristors [15]–[17].

In memristive neuromorphic circuits, the memristor is mostly used as the storage medium to represent a weight. It mainly functions as a neural synapse, and its function is equivalent to that of a single-layer perceptron [18]. The memristor can greatly reduce the power consumption of such neuromorphic networks and the size occupied by the original circuit to improve the efficiency of the network, making it an excellent device for accelerated calculations [19], [20].

Different applications require memristor devices with different physical mechanisms, such as Conductive Bridge RAM (CBRAM), Ferroelectric RAM (FeRAM), Phase Change Memory (PCM), Spin Torque Transfer (STT) MRAM [21], [22]. CBRAM devices are showcasing the most enticing characteristics for a resistive non-volatile memory and computing element [23]–[25]. For the design of circuits based on CBRAMs, appropriate models based on their physical phenomena [26], [27] are required to perform accurate circuit simulations. These models should be compatible with the circuit description as well as their calibration by the experimental response of memristive devices to spike-like signals [28].

Chemical reactions can also showcase qualitatively similar evolution as nerve cells, usually through the chemical information processing activity of the well-known Belousov–Zhabotinsky (BZ) reaction [29]–[31]. There are different reagents in this reaction; activators, which can grow autocatalytically at the appropriate conditions, and inhibitors, which are responsible for suppressing the production of ac-

tivators. The BZ medium utilizes oscillations and spikes to perform operations that can be triggered and activated through the reagents, i.e., the concentration of activators exceeds a threshold value or the concentration of inhibitors falls below a certain level [32]–[34], which can be mapped to the behavior of a neuron.

In this work, taking inspiration from the chemical medium evolution, memristive devices have been used in order to create a neuromorphic *MRC* oscillator. A realistic physical-based memristor model was used, fitted to fabricated CBRAM devices that exhibit both unipolar and bipolar switching behavior under different applied voltage [17]. The unipolar behavior of the CBRAM devices was exploited to reproduce neuron-like oscillations while the bipolar behavior was utilized to implement the synaptic weights of the neuron in a crossbar configuration. The proposed circuitry was able to showcase biological-like behavior and to resolve the XOR problem with a single memristive neuron-like oscillating circuit.

II. MEMRISTIVE DEVICES AND MODEL

A single-layer MIM CBRAM device (Fig. 1(a)) in Ag (~ 40 nm) / SiO₂ (~ 20 nm) / Pt NPs (~ 5 nm) architecture was fabricated in order to develop the proposed chemically-inspired memristor-based neuron-like oscillating circuit. Regarding the fabrication process, thin film depositions on previously oxidized silicon substrates were performed using the RF magnetron sputtering method. A high purity ceramic target (SiO₂ target – 99.99%) was used during the deposition of the 20 nm SiO₂ thin layer. The TiN bottom electrode and Ag top electrode were deposited from respective TiN and Ag sputtering targets, respectively, with a total thickness of 40 nm. Pt NPs were deposited from a high purity Pt target (99.99%) using a novel gas condensation method. The fabricated device shows fast unipolar switching behavior, which is crucial for achieving the desired oscillation. At the same time, this device can showcase bipolar behavior under a higher voltage supply, which is optative in order to be used as neuron weights.

Regarding the realistic physical-based memristor model, it takes into consideration the drift, diffusion, and thermo-diffusion effects to implement the switching dynamics of the memristor. The model is CBRAM based, meaning that the change in resistance is attributed to a conductive filament that is forming and rupturing between the top and bottom electrodes. The thermo-diffusion mechanism will assist in countering the effects of drift and Fick diffusion fluxes, and will contribute to integrating the nanosecond-based switching times of the CF in the model. The switching effect in CF causes large current densities and enhanced local temperature distributions, which lead to enhanced atom migration and thermophoresis [35], [36]. The temperature gradient is a key driver of the switching effect, which is why it's important to include these effects in a model of the switching effect [37], [38]. The model has been developed in Verilog-A in order to enable large-scale circuit simulations.

Regarding the mathematical description of the model's equation set, the state variable is the effective diameter (ϕ)

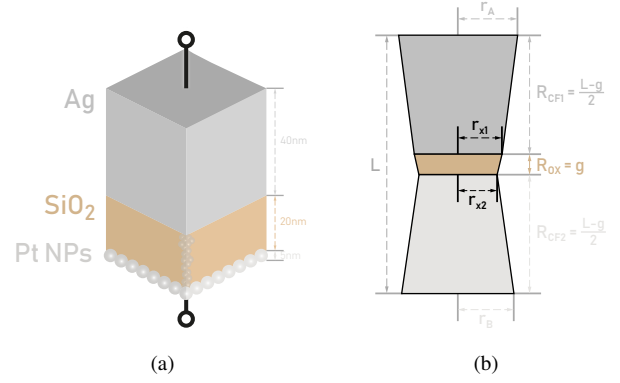


Fig. 1. (a) Fabricated CBRAM device structure. (b) Physical memristor model geometry.

and its derivative is extracted through drift, diffusion, and thermo-diffusion, three effects that are voltage and temperature dependent.

$$\frac{d\phi}{dt} \Big| = \frac{d\phi}{dt} \Big|_{\text{drift}} + \frac{d\phi}{dt} \Big|_{\text{diff}} + \frac{d\phi}{dt} \Big|_{\text{thermo-diff}} = Ae^{-A_{\text{exp}} \frac{E_{\text{drift}} - \alpha q \psi}{k_B T}} + B\phi^{-1} e^{-\frac{E_{\text{diff}}}{k_B T}} - C\phi^{-1} S \left(\frac{T_{\text{hot}} - T_{\text{cold}}}{L/2} \right) \quad (1)$$

The temperature T is calculated through a lumped thermal model which is dependent on the applied voltage V , the resistance of the device R , as well as the effective diameter of the filament.

$$\frac{dT_{\{\text{hot}, \text{cold}\}}}{dt} + \frac{T_{\{\text{hot}, \text{cold}\}} - T_0}{\tau_{\text{th}}} = \frac{|V \times I|}{k_{\text{th}\{\text{hot}, \text{cold}\}}} \quad (2)$$

The resistance of the device R is calculated based on the geometry of two adjoined truncated cone-shaped filaments (Fig. 1(b)), whose size changes according to the effective diameter (ϕ).

$$R = R_{\text{CF1}} + R_{\text{OX}} + R_{\text{CF2}} = \rho_{\text{CF}} \frac{(L-g)/2}{\pi r_A r_{x1}} + \rho_{\text{OX}} \frac{g}{\pi r_{x1} r_{x2}} + \rho_{\text{CF}} \frac{(L-g)/2}{\pi r_B r_{x2}} \quad (3)$$

III. NEURON - CIRCUIT ANALOGY

Neuron cells are in charge of receiving input from the outside world as well as processing and transmitting it [39]. Dendrites, axon, and soma are the three major components of a neuron (Fig. 2). A dendrite is where a neuron receives and processes messages from other neurons' axons. The axon is the neuron's output structure, where it sends information to other neurons via action potentials and connects to the cell body via a specialized junction known as the axon hillock. The soma is the core component of the neuron that houses its genetic information and is essential for maintaining its structure as well as providing energy to drive activity. Finally, the communication link between the axon of one neuron and the dendrite of another is called a synapse.

The brain has billions of neurons, making it a formidable challenge to achieve artificial intelligence by simulating their

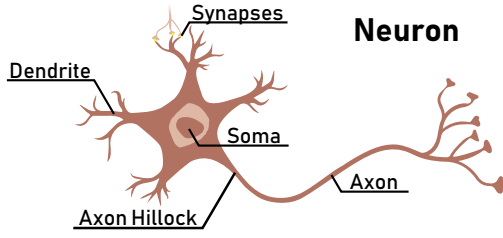


Fig. 2. Biological neuron representation.

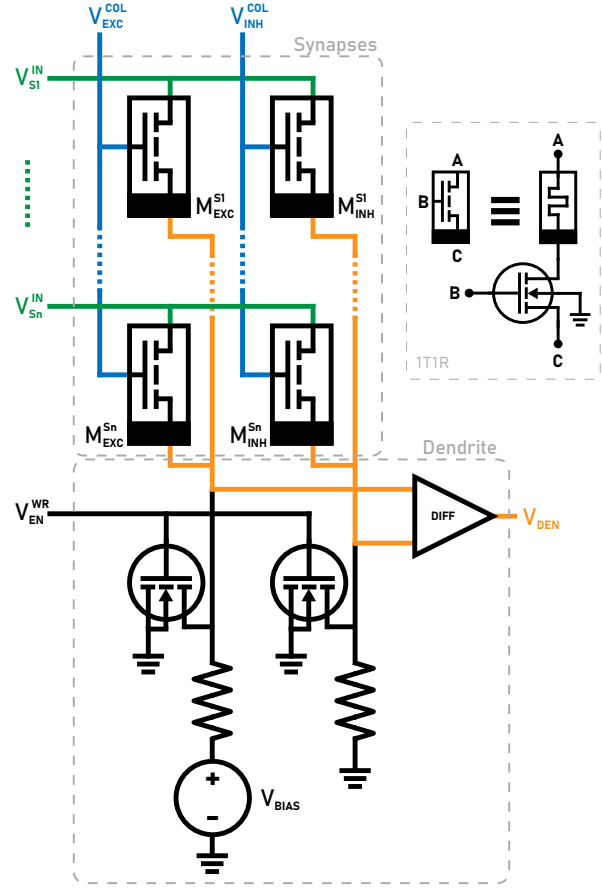
functions. This is why scientists are continuing to improve on neuron-like circuit designs in order to create more realistic and useful devices. Taking inspiration from the biological neuron an oscillating circuit has been designed that mimics its behavior and structure. The proposed neuron-like oscillating circuit takes advantage of memristors in an oscillating manner similar to how nerve cells oscillate inside a biological organism. This allows it to continuously capture and incorporate slow patterns of neural-like activity while also responding quickly to sudden changes in stimulus conditions.

In the proposed neuron-like oscillating circuit, the synapses and the dendrite are represented by bipolar memristors in a crossbar configuration that are able to receive signals from external inputs and other similar neuron-like oscillating circuits (Fig. 3(a)). The soma of the circuit is considered the power supply necessary to send its action potential through its axon. The axon contains an *MRC* oscillator, which is triggered when the weighted sum of the input signals exceed a pre-defined threshold in order to transmit a signal to the following neuron-like oscillating circuits (Fig. 3(b)). This transmitted signal matches the characteristics of biological electric signals called action potentials. The overall system matched the functionality of a biological neuron and can be considered as the first step towards the development of low-power oscillation-based neuromorphic hardware with biological-like behavior.

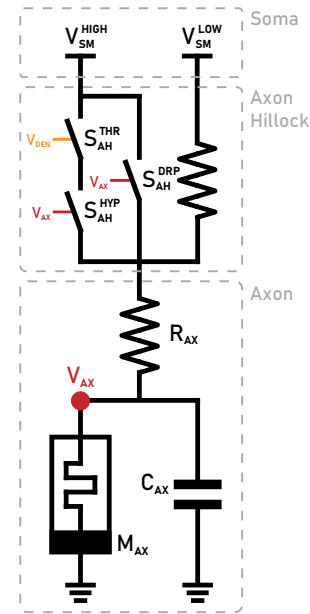
A. Synapses and Dendrite Equivalents Operation

Synapses are represented by CBRAM devices with bipolar behavior in a crossbar configuration in order to be able to incorporate both write/train and read/operation features. The dendrite connects the memristors and a power supply with a switch on the axon hillock. The functionality is similar to a perceptron, with the bias signal being considered the power supply.

Regarding the synapses representation, a $n \times 2$ memristor crossbar is utilized as depicted in Fig. 3(a) with n to be the inputs and 2 to be the two different types of signals that can be observed in a biological neuron; the excitatory ones and the inhibitory ones. The first are used to enable the oscillation, while the second are used to delay it. The memristors are in series with a transistor on a 1T1R topology in order to act as column selectors during the write/train phase. Thus, different numbers of activated pre-neuron-like oscillators lead



(a)



(b)

Fig. 3. (a) Synapses and dendrite circuit equivalent. (b) Soma and axon circuit equivalent.

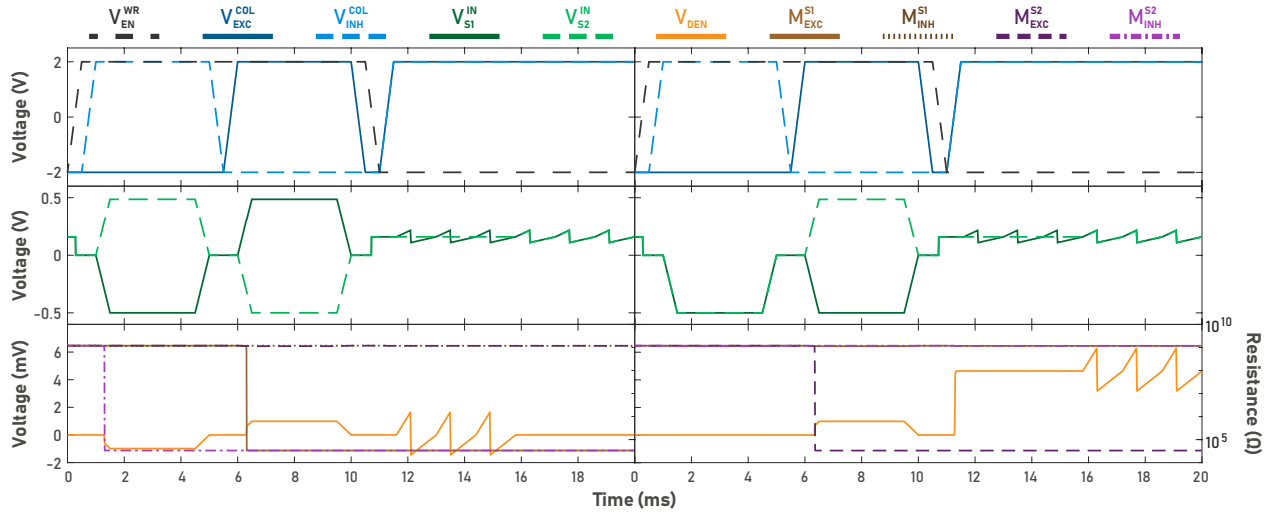


Fig. 4. Operation of the synapses and dendrite circuit equivalents for two different examples.

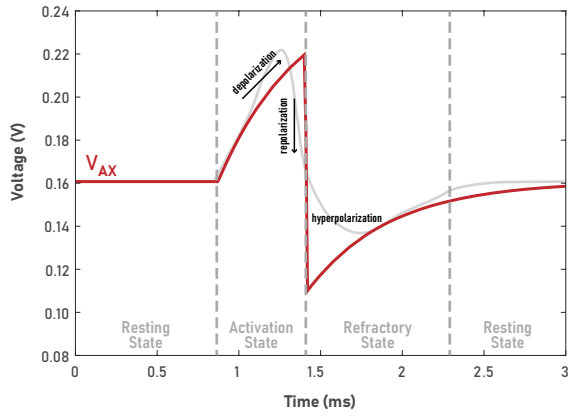


Fig. 5. Action potential-like signal V_{AX} produced by the neuron-like oscillator. Biological neuron action potential representation in light gray.

to different voltage levels on the axon hillock equivalent, depending on the weights of the memristors on the crossbar.

As far as the dendrite equivalent circuit, each of the excitatory and the inhibitory lines is connected to a resistance and to a transistor responsible for grounding the output during the write/train phase. On the excitatory line, a power supply is connected to act as a bias during the read/operational phase of the neuron-like oscillator. The dendrite circuit is responsible for calculating the weighted sum of the input signals depending on the resistance values of the memristors and subtracting the excitatory line from the inhibitory one in order to provide the axon hillock circuit with the final result.

The write/train under two different weight cases can be observed in Fig. 4 under zero bias ($V_{BIAS} = 0V$), as well as the read/operation phase output. The write/train of the neurons take place in the beginning separately for each column. Focusing on the first example (left part), the first neuron is trained in positive/excitatory weight, while the second one in negative/inhibitory weight. In case the input

voltage is positive (e.g. V_{S2}^{IN} at 1 to 5ms), then the respective memristor switches to its low resistance state (e.g. M_{INH}^{S2} at about 1.5ms). Afterwards, the read/operation phase take place (i.e. when $V_{EN}^{WR} = -2V$) when the input oscillating signals are sent for cases $\{S1, S2\} = \{1, 0\}$ and $\{1, 1\}$. For different inputs, different V_{DEN} levels can be observed with the inhibitory action to be clearly spotted when both inputs are present (i.e. $V_{DEN} = 0$ after 16ms). Regarding the second example (right part), the first memristor is trained as inactive (i.e. both memristors M_{EXC}^{S1} and M_{INH}^{S1} at high resistance state) and the second one at positive/excitatory weight, and thus different output is observed at V_{DEN} .

B. Soma and Axon Equivalents Operation

The axon of the neuron-like oscillator produces an oscillation (Fig. 5) known as an action potential in biological neuroscience. In order to achieve this signal, a CBRAM device with unipolar switching dynamics is utilized in combination with a resistor and a capacitor in order to take advantage of the charging and discharging behavior of an RC circuit.

More specifically, the memristor (M_{AX}) oscillates between V_{AX}^{SET} and V_{AX}^{RESET} under constant DC voltage only if the capacitor C_{AX} and the resistor R_{AX} are selected properly in order to avoid the equilibrium point in which no further memristor switch will be possible. In general, the capacitor is responsible for the oscillation time duration, while the resistor can adjust the voltage divider V_{AX} along with the memristor M_{AX} which is the focal point for avoiding the mentioned equilibrium. In detail, the following (in)equations for the V_{AX} divider should be followed during the design phase:

$$V_{AX}^{LOW} = V_{AX}^{RESET} \cdot \frac{R_{AX} + M_{AX}^{LOW}}{M_{AX}^{LOW}} \quad (4)$$

$$V_{AX}^{HIGH} = V_{AX}^{SET} \cdot \frac{R_{AX} + M_{AX}^{HIGH}}{M_{AX}^{HIGH}} \quad (5)$$

$$V_{AX}^{LOW} < V_{AX} < V_{AX}^{HIGH} \quad (6)$$

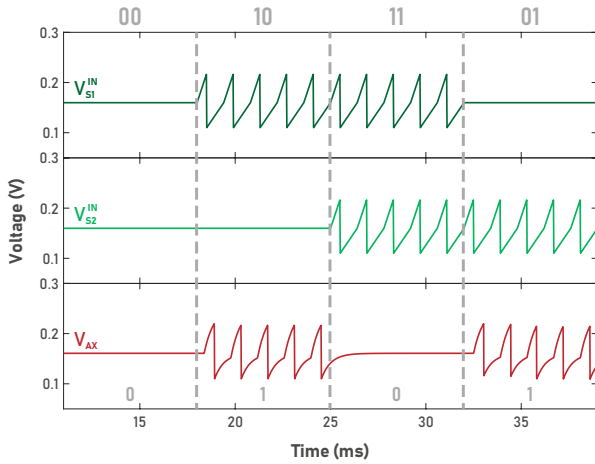


Fig. 6. Output signal V_{AX} for all possible inputs of the XOR gate.

The eq. 4 is valid when the memristor is at *SET* state, where the voltage V_{AX} across the memristor terminals slowly decreases to V_{AX}^{RESET} . In order for the memristor's *RESET* process to get triggered, the eq. 6 should be followed in order to avoid the oscillator reaching equilibrium. Afterwards, the eq. 5 describes the new equilibrium point as the memristor is at its *RESET* state and the voltage V_{AX} slowly increases to V_{AX}^{SET} . Following the eq. 6, the *SET* state can be triggered before the equilibrium is reached, and thus a continuous oscillation between V_{AX}^{SET} and V_{AX}^{RESET} can be achieved.

Before the oscillator, the axon hillock and the soma equivalent circuit can be spotted in Fig. 3(b). More specifically, the voltage supplies V_{SM}^{HIGH} and V_{SM}^{LOW} are responsible for providing the necessary power to the neuron-like oscillator in order to be able to produce the oscillations following the soma function of a biological neuron. The axon hillock equivalent circuit consists of two branches; one for ensuring that the neuron-like oscillator remains at an idle state, while the other controls the oscillation initialization in case the threshold has been reached and ensures a successful oscillating operation.

In more detail, the S_{AH}^{THR} switch is activated when the threshold from the dendrite inputs is reached to activate the oscillation. For the successful operation of the neuron-like oscillator, the S_{AH}^{DRP} switch is introduced to avoid an abrupt interruption of the oscillation and to ensure the successful depolarization and repolarization of the action potential-like oscillating signal. The S_{AH}^{HYP} switch is also included to depict the hyperpolarization period of an action potential.

The operation of the neuron-like oscillating circuit can be divided into three states matching the operation of a biological neuron as shown in Fig. 5. The first is the resting state, in which the oscillator is ready to be activated. The second is the activation state, which occurs when the required threshold is reached and the oscillation begins. The refractory state occurs when the oscillation has achieved lower voltage levels than the resting state. The neuron-like oscillator can only be activated during a resting state, while the others ensure that the action potential-like signal runs properly.

IV. THE XOR PARADIGM

A number of applications can be deployed using the proposed neuron-like oscillator. The application of interest could be fed into a network of such oscillators, where the particular memristor-based neuron can be used to store the required weights and analyze the input data. One such application could be to detect and recognize patterns in data, and then generate new ones based on the detected patterns.

To showcase the computational capabilities of the proposed circuit and as a proof of concept of its functionality, the XOR problem will be addressed. The XOR is one of numerous logical gates that, when operated on binary inputs, produce output for different input combinations but no output for the same inputs (Table I). The outputs of the XOR logic are not linearly separable in the hyperplane, which means that the outputs cannot be classified only by one line able to separate the input data points. For logical gate operations, gates such as AND or OR are linearly separable. Consequently, it usual for most implementations of neural networks to utilize at least 3 neurons to simulate the XOR gate.

TABLE I
XOR GATE TRUTH TABLE

INPUTS		OUTPUT
$S1$	$S2$	AX
0	0	0
0	1	1
1	0	1
1	1	0

In the case of the proposed circuit, only one neuron-like oscillating circuit is sufficient for the implementation of XOR gate. The first input is considered as excitatory, while the second one as inhibitory following the write/train procedure of Fig. 4(left). The output signal V_{AX} of the oscillator can be spotted in Fig. 6 as extracted from simulations of the proposed circuit in Cadence®Virtuoso®. The simulation results proves that the proposed neuron-like circuit was able to produce oscillations only when the inputs are different following the truth table of Table I.

V. CONCLUSIONS

In this work, a chemically-inspired memristor-based neuron-like oscillating circuit has been proposed utilizing fabricated low-voltage CBRAM devices with both unipolar and bipolar behavior, which were simulated with a compact physical CBRAM model and fitted to perform similar behavior. The proposed neuron-like oscillator was able to match different parts of the circuit into the different parts of a biological neuron and to match its output signal to the common action potential of the neuroscience field. Finally, the XOR problem was successfully addressed by utilizing one such neuron-like oscillator. In future work, an interconnected network of neuron-like oscillating circuits will be exploited, among others, for pattern recognition. Also, the further improvement of the circuit operation performance along with the reduction of the

required circuit area will be explored aiming to achieve the requested robustness for various engineering applications.

REFERENCES

- [1] D. Ielmini and S. Ambrogio, "Emerging neuromorphic devices," *Nanotechnology*, vol. 31, no. 9, p. 092001, dec 2019.
- [2] L. Chua, G. C. Sirakoulis, and A. Adamatzky, Eds., *Handbook of Memristor Networks*. Springer, Cham, 2019. [Online]. Available: <https://link.springer.com/book/10.1007/978-3-319-76375-0>
- [3] D. B. Strukov, "Smart connections," *Nature*, vol. 476, no. 7361, pp. 403–405, Aug 2011.
- [4] D. Silver, A. Huang, C. J. Maddison, A. Guez, L. Sifre, G. van den Driessche, J. Schrittwieser, I. Antonoglou, V. Panneershelvam, M. Lanctot, S. Dieleman, D. Grewe, J. Nham, N. Kalchbrenner, I. Sutskever, T. Lillicrap, M. Leach, K. Kavukcuoglu, T. Graepel, and D. Hassabis, "Mastering the game of go with deep neural networks and tree search," *Nature*, vol. 529, no. 7587, pp. 484–489, Jan 2016.
- [5] G. Indiveri, B. Linares-Barranco, T. Hamilton, A. van Schaik, R. Etienne-Cummings, T. Delbruck, S.-C. Liu, P. Dudek, P. Häfliger, S. Renaud, J. Schemmel, G. Cauwenberghs, J. Arthur, K. Hynna, F. Folowosele, S. SAÏGHI, T. Serrano-Gotarredona, J. Wijekoon, Y. Wang, and K. Boahen, "Neuromorphic silicon neuron circuits," *Frontiers in Neuroscience*, vol. 5, 2011.
- [6] S. K. Esser, P. A. Merolla, J. V. Arthur, A. S. Cassidy, R. Appuswamy, A. Andreopoulos, D. J. Berg, J. L. McKinstry, T. Melano, D. R. Barch, C. di Nolfo, P. Datta, A. Amir, B. Taba, M. D. Flickner, and D. S. Modha, "Convolutional networks for fast, energy-efficient neuromorphic computing," *Proceedings of the National Academy of Sciences*, vol. 113, no. 41, pp. 11 441–11 446, 2016.
- [7] M.-K. Kim, Y. Park, I.-J. Kim, and J.-S. Lee, "Emerging materials for neuromorphic devices and systems," *iScience*, vol. 23, no. 12, p. 101846, 2020.
- [8] J. Tang, F. Yuan, X. Shen, Z. Wang, M. Rao, Y. He, Y. Sun, X. Li, W. Zhang, Y. Li *et al.*, "Bridging biological and artificial neural networks with emerging neuromorphic devices: fundamentals, progress, and challenges," *Advanced Materials*, vol. 31, no. 49, p. 1902761, 2019.
- [9] J. Zhu, T. Zhang, Y. Yang, and R. Huang, "A comprehensive review on emerging artificial neuromorphic devices," *Applied Physics Reviews*, vol. 7, no. 1, p. 011312, 2020.
- [10] I.-A. Fyrigos, V. Ntinis, N. Vasileiadis, G. C. Sirakoulis, P. Dimitrakis, Y. Zhang, and I. G. Karafyllidis, "Memristor crossbar arrays performing quantum algorithms," *IEEE Transactions on Circuits and Systems I: Regular Papers*, vol. 69, no. 2, pp. 552–563, 2021.
- [11] T. P. Chatzinikolaou, I.-A. Fyrigos, V. Ntinis, S. Kitsios, M.-A. Tsompanas, P. Bousoulas, D. Tsoukalas, A. Adamatzky, and G. C. Sirakoulis, "Chemical wave computing from labware to electrical systems," *Electronics*, vol. 11, no. 11, 2022.
- [12] R. Tetzlaff, *Memristors and Memristive Systems*, ser. SpringerLink : Bücher. Springer New York, 2013.
- [13] T. P. Chatzinikolaou, I.-A. Fyrigos, V. Ntinis, S. Kitsios, P. Bousoulas, M.-A. Tsompanas, D. Tsoukalas, A. Adamatzky, and G. C. Sirakoulis, "Wave cellular automata for computing applications," in *2022 IEEE International Symposium on Circuits and Systems (ISCAS)*, 2022, pp. 1–5.
- [14] T. P. Chatzinikolaou, I.-A. Fyrigos, and G. C. Sirakoulis, "Image shifting tracking leveraging memristive devices," in *2022 11th International Conference on Modern Circuits and Systems Technologies (MOCASST)*, 2022, pp. 1–4.
- [15] A. Huang, X. Zhang, R. Li, and Y. Chi, "Memristor neural network design," in *Memristor and Memristive Neural Networks*, A. P. James, Ed. Rijeka: IntechOpen, 2017, ch. 12.
- [16] A. Ascoli, I. Messaris, R. Tetzlaff, and L. O. Chua, "Theoretical foundations of memristor cellular nonlinear networks: Stability analysis with dynamic memristors," *IEEE Transactions on Circuits and Systems I: Regular Papers*, vol. 67, no. 4, pp. 1389–1401, 2019.
- [17] P. Bousoulas, S. Kitsios, T. P. Chatzinikolaou, I.-A. Fyrigos, V. Ntinis, M.-A. Tsompanas, G. C. Sirakoulis, and D. Tsoukalas, "Material design strategies for emulating neuromorphic functionalities with resistive switching memories," *Japanese Journal of Applied Physics*, vol. 61, no. SM, p. SM0806, aug 2022.
- [18] L. Ye, Z. Gao, J. Fu, W. Ren, C. Yang, J. Wen, X. Wan, Q. Ren, S. Gu, X. Liu, X. Lian, and L. Wang, "Overview of memristor-based neural network design and applications," *Frontiers in Physics*, vol. 10, 2022.
- [19] C. Tsioustas, P. Bousoulas, J. Hadfield, T. P. Chatzinikolaou, I.-A. Fyrigos, V. Ntinis, M.-A. Tsompanas, G. C. Sirakoulis, and D. Tsoukalas, "Simulation of low power self-selective memristive neural networks for in situ digital and analogue artificial neural network applications," *IEEE Transactions on Nanotechnology*, vol. 21, pp. 505–513, 2022.
- [20] A. Ascoli, R. Tetzlaff, S.-M. S. Kang, and L. Chua, "System-theoretic methods for designing bio-inspired mem-computing memristor cellular nonlinear networks," *Frontiers in Nanotechnology*, vol. 3, p. 7, 2021.
- [21] I. H. Im, S. J. Kim, and H. W. Jang, "Memristive devices for new computing paradigms," *Advanced Intelligent Systems*, vol. 2, no. 11, p. 2000105, 2020.
- [22] IRDS, "IEEE International Roadmap for Devices and Systems: Beyond CMOS," 2021.
- [23] Z. Wang, C. Li, W. Song, M. Rao, D. Belkin, Y. Li, P. Yan, H. Jiang, P. Lin, M. Hu *et al.*, "Reinforcement learning with analogue memristor arrays," *Nature Electronics*, vol. 2, no. 3, pp. 115–124, 2019.
- [24] L. Xia, P. Gu, B. Li, T. Tang, X. Yin, W. Huangfu, S. Yu, Y. Cao, Y. Wang, and H. Yang, "Technological exploration of rram crossbar array for matrix-vector multiplication," *Journal of Computer Science and Technology*, vol. 31, no. 1, pp. 3–19, 2016.
- [25] C. Li, M. Hu, Y. Li, H. Jiang, N. Ge, E. Montgomery, J. Zhang, W. Song, N. Dávila, C. E. Graves *et al.*, "Analogue signal and image processing with large memristor crossbars," *Nature Electronics*, vol. 1, no. 1, p. 52, 2018.
- [26] P. Bousoulas, D. Sakellaropoulos, C. Papakonstantinopoulos, S. Kitsios, C. Arvanitis, E. Bagakis, and D. Tsoukalas, "Investigating the origins of ultra-short relaxation times of silver filaments in forming-free SiO₂-based conductive bridge memristors," *Nanotechnology*, vol. 31, no. 45, p. 454002, 2020.
- [27] I.-A. Fyrigos, T. P. Chatzinikolaou, V. Ntinis, S. Kitsios, P. Bousoulas, M.-A. Tsompanas, D. Tsoukalas, A. Adamatzky, A. Rubio, and G. C. Sirakoulis, "Compact thermo-diffusion based physical memristor model," in *2022 IEEE International Symposium on Circuits and Systems (ISCAS)*, 2022, pp. 1–5.
- [28] D. Zhevenko, F. Meshchaninov, V. Kozhevnikov, E. Shamin, A. Belov, S. Gerasimova, D. Guseinov, A. Mikhaylov, and E. Gornev, "Simulation of memristor switching time series in response to spike-like signal," *Chaos, Solitons & Fractals*, vol. 142, p. 110382, 2021.
- [29] J. Gorecki and J. N. Gorecka, "Information processing with chemical excitations—from instant machines to an artificial chemical brain," *International Journal of Unconventional Computing*, vol. 2, no. 4, 2006.
- [30] P. L. Gentili, V. Horvath, V. K. Vanag, and I. R. Epstein, "Belousov-Zhabotinsky "chemical neuron" as a binary and fuzzy logic processor," *IJUC*, vol. 8, no. 2, pp. 177–192, 2012.
- [31] J. Stovold and S. O'Keefe, "Simulating neurons in reaction-diffusion chemistry," in *International Conference on Information Processing in Cells and Tissues*. Springer, 2012, pp. 143–149.
- [32] A. Adamatzky, B. D. L. Costello, and T. Asai, *Reaction-diffusion computers*. Elsevier, 2005.
- [33] A. Zaikin and A. Zhabotinsky, "Concentration wave propagation in two-dimensional liquid-phase self-oscillating system," *Nature*, vol. 225, no. 5232, pp. 535–537, 1970.
- [34] A. Zhabotinsky and A. Zaikin, "Autowave processes in a distributed chemical system," *Journal of theoretical biology*, vol. 40, no. 1, pp. 45–61, 1973.
- [35] D. B. Strukov, F. Alibart, and R. S. Williams, "Thermophoresis/diffusion as a plausible mechanism for unipolar resistive switching in metal-oxide-metal memristors," *Applied Physics A*, vol. 107, no. 3, pp. 509–518, 2012.
- [36] A. Marchewka, B. Roesgen, K. Skaja, H. Du, C.-L. Jia, J. Mayer, V. Rana, R. Waser, and S. Menzel, "Nanoionic resistive switching memories: On the physical nature of the dynamic reset process," *Advanced Electronic Materials*, vol. 2, no. 1, p. 1500233, 2016.
- [37] J. M. Goodwill, G. Ramer, D. Li, B. D. Hoskins, G. Pavlidis, J. J. McClelland, A. Centrone, J. A. Bain, and M. Skowronski, "Spontaneous current constriction in threshold switching devices," *Nature communications*, vol. 10, no. 1, pp. 1–8, 2019.
- [38] J. Yoo, I. Karpov, S. Lee, J. Jung, H. S. Kim, and H. Hwang, "Threshold voltage drift in Te-based ovonic threshold switch devices under various operation conditions," *IEEE Electron Device Letters*, vol. 41, no. 1, pp. 191–194, 2019.
- [39] J. G. Nicholls, A. R. Martin, B. G. Wallace, and P. A. Fuchs, *From neuron to brain*. Sinauer Associates Sunderland, MA, 2001, vol. 271.